CONCLUSION

The investigated ^{99m}Tc-labeled endothelin derivative allows screening of atherosclerosis in animals. The accumulation of the endothelin derivative in induced atherosclerotic lesions correlates with the neointimal amount of smooth muscle cells. Therefore, the endothelin derivative may be useful in gaining information on the cellular composition or the proliferative status of atherosclerotic lesions.

ACKNOWLEDGMENTS

The authors thank Eva Maria Bickel and Ingolf Weber for their excellent technical assistance. A preliminary account of this work was published in abstract form (*5*).

REFERENCES

1. Ross R. The pathogenesis of atherosclerosis: a perspective for the 1990s. *Nature* 1993;362:801–809.
2. Hanke H, Strohschneider T, Oberhoff M, Betz E, Karsch KR. Time course of smooth muscle cell proliferation in the intima and media of arteries following experimental angioplasty. *Circ Res* 1990;67:651–659.
3. Sakurai T, Yanagisawa M, Masaki T. Molecular characterization of endothelin receptors. *Trends Pharmacol Sci* 1992;13:103–108.
4. Takuwa Y, Kasuya Y, Takuwa N, et al. Endothelin receptor is coupled to phospholipase C via a pertussis toxin-insensitive guanine nucleotide-binding regulatory protein in vascular smooth muscle cells. *J Clin Invest* 1990;85:653–658.
5. Dinkelborg LM, Duda S, Hanke H, Tepe G, Hilger CS, Semmler W. Characterization of a technetium-99m-endothelin derivative for imaging of atherosclerosis in a rabbit balloon denudation model. *J Nucl Med* 1997;38(suppl):173P.
6. Doherty AM, Cody WL, DePue PL, et al. Structure-activity relationships of C-terminal endothelin hexapeptide antagonists. *J Med Chem* 1993;36:2585–2594.
7. Johannsen B, Jankowsky R, Noll B, et al. Technetium coordination ability of cysteine-containing peptides: x-ray absorption spectroscopy of a ^{99}Tc-labelled endothelin derivative. *Appl Radiat Isot* 1997;48:1045–1050.
8. Rubanyi GM, Polokoff MA. Endothelins: molecular biology, biochemistry, pharmacology, physiology, and pathophysiology. *Pharmacol Rev* 1994;46:325–415.
9. Goto K, Warner TD. Molecular pharmacology. Endothelin versatility. *Nature* 1995; 375:539–540.
10. Lerman A, Edwards BS, Hallett JW, Heublein DM, Sandberg SM, Burnett JC Jr. Circulating and tissue endothelin immunoreactivity in advanced atherosclerosis. *N Engl J Med* 1991;325:997–1001.
11. Tahara A, Kohno M, Yanagi S, et al. Circulating immunoreactive endothelin in patients undergoing percutaneous transluminal coronary angioplasty. *Metabolism* 1991;40:1235–1237.
12. Zeiher AM, Goebel H, Schachinger V, Ihling C. Tissue endothelin-1 immunoreactivity in the active coronary atherosclerotic plaque. A clue to the mechanism of increased vasoreactivity of the culprit lesion in unstable angina. *Circulation* 1995;91:941–947.
13. Hirata Y, Takagi Y, Fukuda Y, Marumo F. Endothelin is a potent mitogen for rat vascular smooth muscle cells. *Atherosclerosis* 1989;78:225–228.
14. Bobik A, Grooms A, Millar JA, Mitchell A, Grinpukel S. Growth factor activity of endothelin on vascular smooth muscle. *Am J Physiol* 1990;258:C408–C415.
15. Wang X, Douglas SA, Louden C, Vickery Clark LM, Feuerstein GZ, Ohlstein EH. Expression of endothelin-1, endothelin-3, endothelin-converting enzyme-1, and endothelin-A and endothelin-B receptor mRNA after angioplasty-induced neointimal formation in the rat. *Circ Res* 1996;78:322–328.
16. Douglas SA, Louden C, Vickery Clark LM, et al. A role for endogenous endothelin-1 in neointimal formation after rat carotid artery balloon angioplasty. Protective effects of the novel nonpeptide endothelin receptor antagonist SB 209670. *Circ Res* 1994;75: 190–197.
17. Winkles JA, Alberts GF, Brogi E, Libby P. Endothelin-1 and endothelin receptor mRNA expression in normal and atherosclerotic human arteries. *Biochem Biophys Res Commun* 1993;191;1081–1088.
18. Kowala MC, Rose PM, Stein PD, et al. Selective blockade of the endothelin subtype A receptor decreases early atherosclerosis in hamsters fed cholesterol. *Am J Pathol* 1995;146:819–826.
19. Ihling C, Gobel HR, Lippoldt A, et al. Endothelin-1-like immunoreactivity in human atherosclerotic coronary tissue: a detailed analysis of the cellular distribution of endothelin-1. *J Pathol* 1996;179:303–308.
20. Dashwood MR, Sykes RM, Muddle JR, et al. Autoradiographic localization of [125I]endothelin binding sites in human blood vessels and coronary tissue: functional correlates. *J Cardiovasc Pharmacol* 1991;17(suppl 7):S458–S462.

Renal Depth Estimates to Improve the Accuracy of Glomerular Filtration Rate

Adam P. Steinmetz, S. Tzila Zwas, Sorina Macadziob, Galina Rotemberg and Ygal Shrem

Department of Nuclear Medicine, Chaim Sheba Medical Center, Tel Hashomer; Sackler School of Medicine, Tel-Aviv University, Tel-Aviv; and Elscint Ltd., Haifa, Israel

This study was performed to validate a computer implementation of the Gates' method for radionuclide glomerular filtration rate (RGFR) calculation. The accuracy of the original method was improved by replacing the Tonnesen formula that estimated renal depth with direct measurement from lateral views to calculate tissue attenuation correction. **Methods:** Both the creatinine clearance test (CCT) and dynamic ^{99m}Tc-diethylenetriamine pentaacetic acid (DTPA) renal scintigraphy (DRS) were performed on 38 patients on the same day. RGFR was quantified from the attenuation corrected absolute DTPA uptake of the kidneys on DRS from 120–180 sec after injection. Attenuation correction was estimated using the lateral views of the kidneys taking in account the distance from the computed geometric center of the kidneys to the posterior body surface along a line vertical to the collimator surface. CCT and glomerular filtration rate estimates from DRS were compared by linear regression. **Results:** RGFR estimates agreed well with CCT, yielding a correlation coefficient of 0.92 in 38 patients and 0.90 in a subgroup of 11 patients suffering from chronic renal failure. **Conclusion:** Present modifications improve RGFR accuracy to the precision range of blood sample based methods. This modified method requires little additional work and no extra cost in patients undergoing DRS. RGFR calculation may be advantageous in cases when 24-hr urine collection for CCT cannot be obtained, and it should improve the accuracy of the captopril test.

Key Words: glomerular filtration rate; kidney radionuclide imaging; technetium-99m-diethylenetriamine pentaacetic acid

J Nucl Med 1998; 39:1822–1825

By the request of a nuclear medicine hardware manufacturer (Elscint, Haifa, Israel) validation of a computer program calculating glomerular filtration rate (GFR) based on the Gates' method (*1–3*) was undertaken. The precision of the original method was significantly improved by replacing the Tonnesen formula by direct measurement of the kidney depth from lateral views, thus improving the accuracy of tissue attenuation correction of the renal uptake.

MATERIALS AND METHODS

Fifty patients were included in the study group (20 women, 30 men; age range 7–84 yr, including 3 children; mean age 44 yr).

Received Nov. 21, 1996; revision accepted Jan. 12, 1998.

For correspondence or reprints contact: S. Tzila Zwas, MD, Department of Nuclear Medicine, Chaim Sheba Medical Center, Tel-Hashomer, Ramat-Gan 52621, Israel.

Clinical renal diagnosis included mainly normals (n = 14), chronic renal failure (n = 11) and others (n = 13) including one patient with one kidney and another one with a transplanted kidney.

Dynamic renal scintigraphy was performed on each patient in a way similar to our standard examinations as detailed later.

Patients were encouraged to drink about 800 cc of fluids 1 hr before the examination. Examinations were performed on a digital gamma camera (Apex SP-4; Elscint, Haifa, Israel) mounted with a low-energy, high-resolution collimator (Elscint APC-4S). A syringe containing 185 MBq (5 mCi) ^{99m}Tc-diethylenetriamine pentaacetic acid (DTPA) was placed on a 30-cm thick styrofoam holder on the surface of the examination table with the camera under the table. An image of the syringe was acquired for 1 min in word mode to avoid pixel overflow.

Each patient was positioned over the camera in a supine position. The counted DTPA dose was injected to an antecubital vein, and a dynamic scan was started in a 128 × 128 frame matrix for the next 20 min divided into three consecutive time intervals. The first interval was of 60 sec duration at a rate of 2 sec per frame, the second for 6 min at 6 sec per frame and the third for the remaining 13 min at 30 sec per frame.

Immediately thereafter, with the patient immobilized, the camera was tilted to the left and right sides of the table, and posterior and two lateral orthogonal renal static images for about 400 kilocounts each were obtained.

The injection site view was also obtained to exclude subcutaneous infiltration of the dose. Finally, the empty syringe was scanned again using the preinjection syringe acquisition parameters. When injection through a butterfly needle was performed, the whole syringe, tubing and needle assembly were counted in the camera field of view for residual activity.

Before the radionuclide study, a blood sample was drawn from each patient for serum creatinine after a 24-hr urine collection for a creatinine clearance test (CCT).

GFR was calculated individually for each kidney according to the Gates' method from the background and attenuation-corrected DTPA uptake from 120–180 sec after tracer arrival to the kidneys. Background was estimated using a semilunar region of interest (ROI) around the lower pole of the kidneys. Tissue attenuation was calculated using the renal depth measured directly from the orthogonal lateral views. The precision of measurement was further optimized by drawing an ROI around the lateral view of the kidney, then finding the geometric center of this ROI with the aid of the computer and, finally, measuring the distance from this point to the posterior body surface along a line perpendicular to the table top (Fig. 1). Obviously in the case of the renal transplant patient, the distance of the transplant from the anterior body surface was measured because the dynamic imaging was performed from the anterior view.

The Tonnesen regression formula used in the original Gates' method (*2*) was excluded because of the calculated high errors in the renal depth estimations as compared with our direct measurements.

Acquisition protocols and postacquisition processing including calculations of GFR were performed on the gamma camera computer by a program written in Elscint's CLIP language. The GFR values obtained from the dynamic renal scans were compared to the biochemical CCT values by simple linear regression. The coefficient of correlation (Pearson's r value) and the s.e.e. for both CCT and GFR were used for evaluation of the validity of our method. The interobserver variation was tested by a paired Student's t-test (*4*).

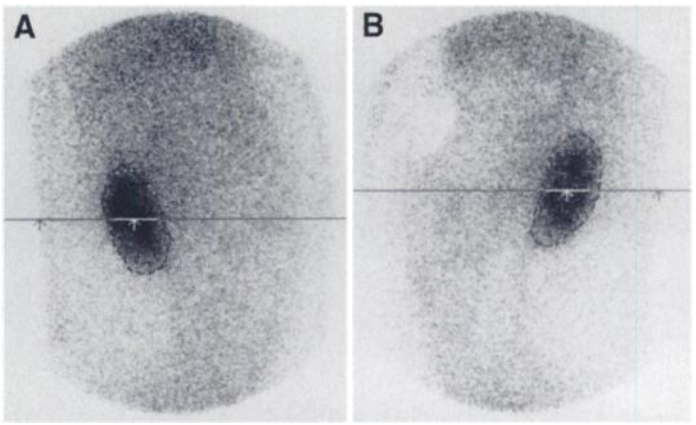

FIGURE 1. A region of interest (ROI) was drawn marking each kidney contour. Renal depth can be accurately estimated from the lateral view. (A) Right kidney, (B) left kidney. Arrow inside this ROI was positioned by computer on its geometric center. Then, the computer drew a line passing point of arrow, perpendicular to surface of the table top (horizontal in this picture). Second arrow was positioned by operator on intersection of this line and posterior body contour. Computer limits movement of second arrow along this line.

RESULTS

Fifty patients were included initially in our study. In 38 of the 50 patients included in the study, both CCT and GFR were fully obtained. The rest of the studies were rejected due to incomplete CCT and equivocal GFR (infiltration at injection site). All CCT and GFR studies were evaluated and calculated results were summarized in Table 1.

As shown in Table 1, linear regression between CCT and GFR yielded a correlation coefficient of 0.92 with the regression equation:

$$CCT = 0.77 \times GFR + 13.4 \qquad \text{Eq. 1}$$

Scatterplot and regression line are seen on Figure 2. To analyze the validity of the Tonnesen's formula, it was compared with directly measured right and left renal depth by our method obtaining relatively low correlation coefficient r equal to 0.75 and 0.78 for the left and right kidneys, respectively, as shown in Figure 3.

In 14 patients considered to have a normal urinary system, GFRs were calculated also using both the original Gates' method and our modified procedure to compare the accuracy of the two techniques. The CCT and the GFR values obtained by both methods are presented in Table 2.

When using direct measurement of renal depth and including it, the calculated Pearson's r correlation coefficient was 0.87. When the same studies were recalculated using only estimated renal depth, this value decreased to 0.51. This is readily explained by the weaker correlation between the estimated and the directly measured renal depth.

An additional subgroup of 11 patients suffering from chronic renal failure was also selected to check the validity of the

TABLE 1
Summarized Creatinine Clearance Test (CCT) and Glomerular Filtration Rate (GFR)

Group	Patient	CCT	GFR	p*
Normals	14	78.1 ± 5.2	75.7 ± 5.1	0.87
CRF	11	32.1 ± 4.0	31.3 ± 4.5	0.90
All	38	66.2 ± 4.6	68.6 ± 5.5	0.92

*p = correlation coefficient CCT vs. GFR.
Data presented as mean ± s.e.e.

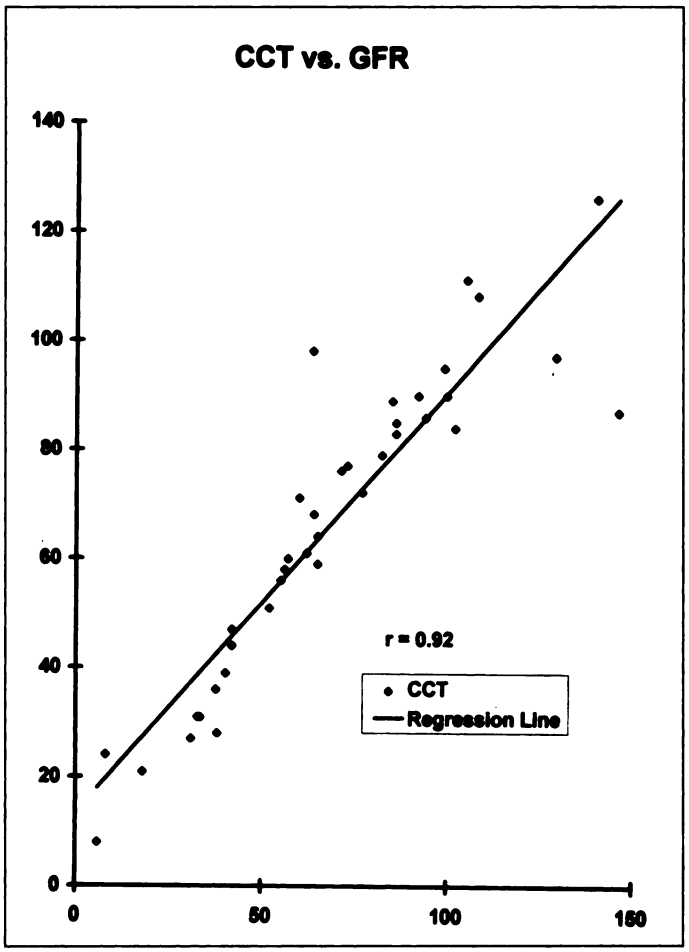

FIGURE 2. Scatterplot and regression line of radionuclide glomerular filtration rate and creatinine clearance test.

improved method under the CRF condition. The linear correlation coefficient in this subgroup between CCT and GFR was 0.90.

To further evaluate the current method's repeatability, the GFR measurements were performed in a subgroup of 19 patients by two independent operators. No significant difference was demonstrated between the two GFR estimates with a repeatability coefficient of 0.06.

TABLE 2
Glomerular Filtration Rate (GFR) Obtained with Measured Depth Correction as Compared to the Original Gates' Method

Patient no.	Creatinine clearance	GFR with measured renal depth	GFR by Gates' estimated renal depth
1	72	77	56
2	60	57	46
3	98	64	43
4	51	52	40
5	86	94	56
6	95	99	105
7	85	86	60
8	68	64	55
9	58	56	48
10	111	105	46
11	64	65	51
12	61	62	35
13	108	108	86
14	76	71	52

DISCUSSION

The original task of this work was the validation of a computer program written for the Gates' method for GFR calculation. In reviewing the relevant literature, it became clear that although the method was simple and promising it had not received widespread acceptance, and its accuracy was criticized frequently (*5–7*).

Our first few GFR estimates using the original protocol yielded inaccurate results when compared to CCT. Meticulous and critical review of the whole procedure including radiopharmaceutical preparation, injection, dynamic scanning and computer processing of the data revealed most of the errors were introduced by the tissue attenuation correction using the Tonnesen formula based estimates of the renal depth. In the patients with malpositioned kidney or with renal transplant, the formula-based estimate of the renal depth was evidently invalid.

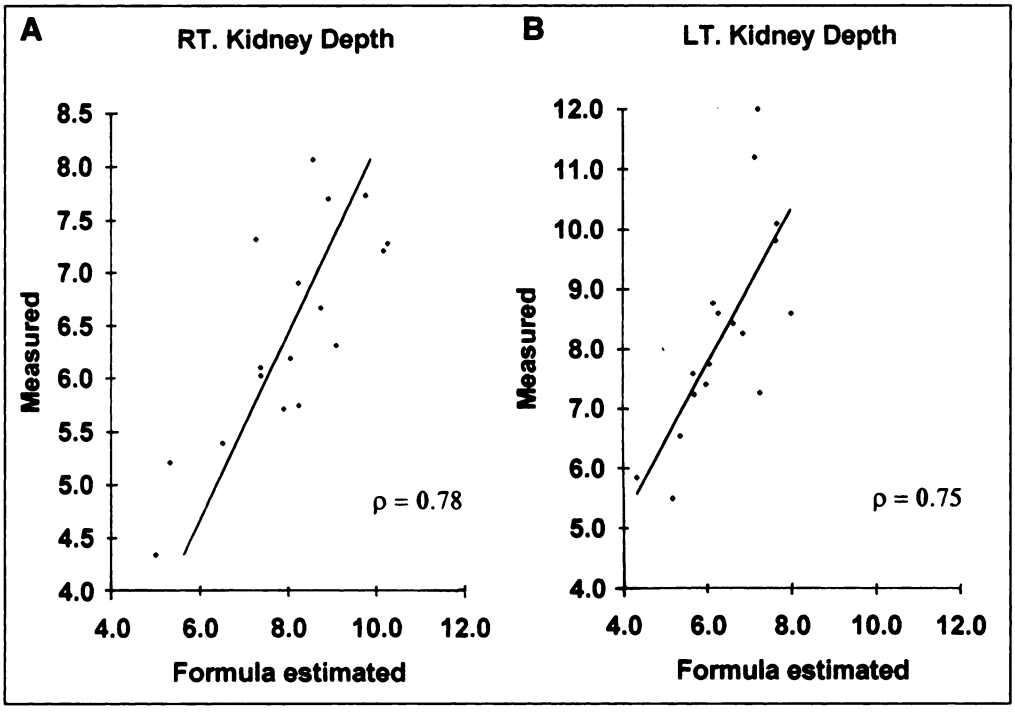

FIGURE 3. Scatterplots and regression lines of the Tonnesen formula calculated renal depths and computer-aided measured values. (A) Right kidney, (B) left kidney.

To overcome this problem, several approaches were considered. The use of another formula for renal depth published by Taylor et al. (*8*) reported to be more precise, but still would not be accurate for a malpositioned kidney or for a renal transplant. In theory, we could refer our patients for ultrasound or CT to measure their renal depth individually, but this idea was rejected because of the additional testing with another imaging modality. Individually measured renal depth was reported to improve the GFR measurements compared with CCT (*9–10*). Due to these reasons, the method of measuring renal depth from lateral scintigrams was adopted. The suggested procedure is confined entirely within the nuclear medicine department without the involvement of other modalities, and inaccuracies introduced by formula-based estimates can be avoided.

Accurately measuring the renal depth on the lateral view still posed some challenges. Initially, the center of kidney was detected through visual inspection, and the shortest distance between this point and the posterior body surface was measured. However, it was difficult to pinpoint the center of the kidneys due to the poor visualization of kidneys on the lateral views obtained 20 min after ^{99m}Tc-DTPA injection. To improve the localization of the center of the kidney, the method of drawing an ROI around the kidney contour on the lateral view was adopted. With some enhancement of the contrast on the computer screen, this could be consistently accomplished.

The direction of the kidney-to-skin line drawn by visual inspection did not necessarily coincide with the direction of the gamma rays forming the posterior view. The computer-generated line is a closer approximation of the distance the gamma rays traveled in the body toward the camera than the shortest line from the center of the kidney to the body surface.

Although beyond the scope of this study, it's important to mention that including the attenuation correction in calculating the split renal function may pose a potential problem. Attenuation correction influences the split renal function, especially in patients with renal malposition. It is obvious that the attenuation-corrected values of the split renal function are more accurate. However, most dynamic renal scintigrams are processed without attenuation correction. Therefore, when reporting renal scintigrams processed with the present modified method, it is strongly suggested to report both attenuation corrected and uncorrected values of split renal function to avoid confusion when comparing results with previous ones obtained without attenuation correction (*11*).

CONCLUSION

Since its initial publication in 1982, the Gates' method for calculating GFR has been praised because of its simplicity and criticized due to its varying accuracy.

The modifications described in this study improve the accuracy of the Gates' method to a precision comparable with the radionuclide methods using blood samples (*12*). These modifications can also handle GFR calculations in patients with renal ectopia or transplants. This method is easy to perform without any inconvenience to the patient and with no extra cost.

GFR measurement by dynamic renal scintigraphy, albeit more expensive than CCT, requires the availability of a nuclear medicine service, needs no 24-hr urine collection and it yields results in the same day. This is advantageous when dealing with outpatients visiting from remote places or in patients for whom 24-hr urine collection is unreliable. Implementing the RGFR direct calculation improves the general diagnostic accuracy of dynamic renal scintigraphy (DRS), particularly the captopril-challenged DRS (*13–15*), in kidneys in the anomalous position, and it should be used routinely in renal scans due to its simplicity and its obvious high accuracy in GFR assessment.

ACKNOWLEDGMENTS

This study was supported in part by the Nuclear Medicine R&D Department, Elscint LTD, Haifa, Israel.

REFERENCES

1. Gates GF. Glomerular filtration rate:estimation from fractional renal accumulation of technetium-99m-DTPA (stannous). *Am J Roentgnol* 1982;138:565–570.
2. Gates GF. Split renal function testing using technetium-99m-DTPA. A rapid technique for determining differential glomerular filtration. *Clin Nucl Med* 1983;9:400–407.
3. Gates GF. Computation of glomerular filtration rate with technetium-99m-DTPA: an in-house computer program. *J Nucl Med* 1984;25:613–618.
4. Bland JM, Altman DG. Statistical methods for assessing agreement between two methods of clinical measurement. *Lancet* 1986;1(8476):307–310.
5. Gruenewald SM, Collins LT, Fawdry RM. Kidney depth measurement and its influence on quantitation of renal function. *Clin Nucl Med* 1985;10:398–401.
6. Maneval DC, Magill HL, Cypess AM, Rodman JH. Measurement of skin-to-kidney distance in children: implications for quantitative renography. *J Nucl Med* 1990;31: 287–291.
7. Awdeh M, Kouris K, Hassan IM, Abdel-Dayem HM. Factors affecting the Gates' measurement of glomerular filtration rate. *Am J Physiol Imaging* 1990;5:36–41.
8. Taylor A, Lewis C, Giacometti A, et al. Improved formulas for the estimation of renal depth in adults. *J Nucl Med* 1993;34:1766–1769.
9. Chachati A, Meyers A, Godon JP, Rigo P. Rapid method for the measurement of differential renal function: validation. *J Nucl Med* 1987;28:829–836.
10. Ginjaume M, Casey M, Barker F, Duffy G. A comparison between four simple methods for measuring glomerular filtration rate using technetium-99m-DTPA. *Clin Nucl Med* 1986;11:647–650.
11. Cosgriff P, Brown H. Influence of kidney depth on the renographic estimation of relative renal function. *J Nucl Med* 1990;31:1576–1577.
12. Waller DG, Keast CM, Fleming JS, Ackery DMI. Measurement of glomerular filtration rate with technetium-99m-DTPA: comparison of plasma clearance techniques. *J Nucl Med* 1987;28:372–377.
13. Chen CC, Hoffer PB, Vahjen G, et al. Patients at high risk for renal artery stenosis: a simple method of renal scintigraphic analysis with technetium-99m-DTPA and captopril. *Radiology* 1990;176:365–370.
14. Cuocolo A, Esposito S, Volpe M, Celentano L, Brunetti A, Salvatore MTI. Renal artery stenosis detection by combined Gates' technique and captopril test in hypertensive patients. *J Nucl Med* 1989;30:51–56.
15. Cuocolo A, Esposito S, Volpe M, Celentano L, Brunetti A, Salvatore M. Renal artery stenosis detection by combined Gates' technique and captopril test in hypertensive patients. *J Nucl Med* 1989;30:1422–1423.